J. Meas. Sci. Instrum., 2024, 15(2): 216-223.
DOI: 10.62756/jmsi.1674-8042.2024022
http://jmsi.publish.founderss.cn
jmsi@nuc.edu.cn

Monocular visual guidance method for terminal docking of an autonomous underwater vehicle

WANG Qiusheng, QI Xiangdong*, XUE Chenyang, LIU Dan, WANG Yonghua, WANG Jingnan

Key Laboratory of Instrumentation Science & Dynamic Measurement of Ministry of Education, North University of China, Taiyuan 030051, China

***Corresponding author:** QI Xiangdong (qixiangdong@nuc.edu.cn)

Received: January 9, 2024 **Revised:** February 5, 2024 **Accepted:** April 2, 2024

Abstract: Efficient recovery of the autonomous underwater vehicle (AUV) in complex underwater environments is a major technological challenge. A terminal docking method using monocular vision was presented to detect and track a circular light source marker at the docking station. To improve the recognition of the light source feature, the Canny edge detection algorithm was improved, the adaptive threshold method was used to dynamically adjust the light source contour, and the minimum enclosing circle method was used to determine the light source center when the threshold was optimal. In addition, geometric position and area constraints were used to eliminate interference from water surface reflections. For visual localization and tracking, Zhang's calibration method was used to obtain the internal and distortion parameters of the camera, yaw and pitch errors of the AUV were estimated by comparing the light source center with the camera image center, then the position-attitude PID controller was used to achieve rapid attitude adjustment. The pool experimental results showed that the approach was simple, practical, and robust, providing a technical reference for future reliable recovery of underwater robots.

Key words: autonomous underwater vehicle (AUV); terminal docking; monocular visual; position estimation; image processing

0 Introduction

The autonomous underwater vehicle (AUV) is intelligent, flexible, and stealthy, making it increasingly prevalent in various fields such as ocean science research, resource exploration, and military reconnaissance[1-3]. However, the AUV is limited by onboard energy reserves and the underwater communication environment, requiring timely recovery for energy replenishment, data upload, and other tasks. Autonomous underwater docking is more convenient than manual salvage on the surface, but terminal docking of the AUV with docking devices remains a technical challenge due to the complexity of the underwater environment[4,5].

Currently, the main methods for achieving terminal docking of the AUV include acoustic, optical, visual, and electromagnetic guidance[6-8]. Due to the advantages of precise positioning, easy deployment, and low cost, visual guidance has gradually become a research hotspot for AUV docking and recovery[9]. Park et al.[10] used a charge-coupled device (CCD) camera to capture a five-light source array marker, using image segmentation and averaging the centers of each light source for plane localization. They successfully dock the ISiMI AUV in a pool, but the detected center of the light source can deviate significantly due to light scattering. Figueiredo et al.[11] determined the centers of three colored ball markers through color segmentation and used quaternion feedback methods for pose estimation. They successfully achieve suspended docking of the MARES AUV in a pool, but the detection distance is limited due to the passive marking mechanism. Palomeras et al.[12] combined light source markers with augmented reality (AR) markers, using AR for continuous guidance when the near light source was out of the camera view. They successfully dock of the Sparus II AUV in a lake. Li et al.[13] used a high-power light source as a docking marker and successfully guided the docking through image denoising, segmentation, and light source center localization in a pool. However, due to the lack of light source feature recognition, the method is susceptible to interference. Liu et al.[14] proposed a docking neural network (DoNN) method, combined with a robust perspective-n-point (RPNP) algorithm, which successfully docked in a lake but required a large amount of prior dataset for light source localization training. Currently, underwater visual

terminal guidance has the limitation of complex positioning, which requires further research on AUV docking technology necessary.

To achieve close docking of the AUV in complex underwater environments, exploring terminal monocular visual guidance methods were focused on. Using a coaxial circular light source at the entrance of the docking station as a docking marker, image processing algorithms was designed and optimized to improve visual detection accuracy and robustness. Additionally, monocular visual coordinates was established for position estimation and docking control strategies was developed to correct for actual position errors. Pool experimental results demonstrated the effectiveness of the proposed approach.

1 Monocular visual system

The underwater docking marker is an important auxiliary equipment in the visual guidance of the AUV. Currently, geometric arrays consisting of multiple independent light sources are widely used, but the design has a high risk of occlusion and malfunction, and the algorithm for identifying and localizing multiple light sources is relatively cumbersome.

In this paper, a single light source is chosen as the docking marker, as shown in Fig. 1. A flexible strip of LED light was wrapped around the entrance of the docking station, and the center of the circular marker was on the same level as the center of the docking station entrance. The brightness of the light source could be adjusted, and a body of water was utilized to absorb less blue light to improve visibility. The device was structured in design, easy to deploy, and reduced the requirement for autonomous docking of the AUV.

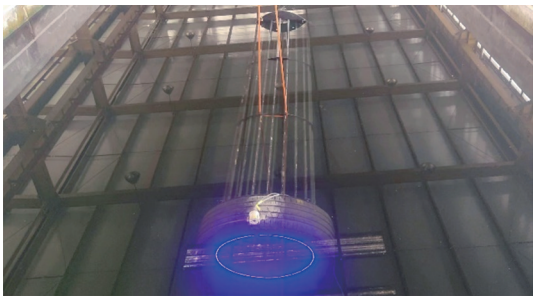

Fig. 1 Light source marker at docking station

The AUV was equipped with a Sony CMOS sensor camera and a resolution of 1 920×1 080 pixels to capture clear underwater image. The CPU of the image processor was i7 5500u, running under a Linux system environment. As shown in Fig. 2, monocular camera localization of a single light source center is implemented in an image processor, the attitude information is transmitted to the main controller via the serial port for analysis and processing, and a set of PWM wave signals are output to coordinate the operation of the four propellers to change the AUV motion attitude.

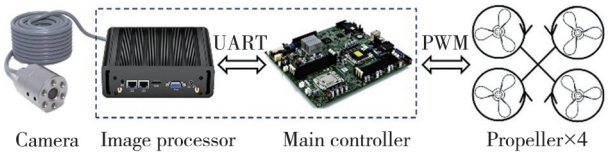

Fig. 2 AUV visual processing system

2 Visual processing methods

2.1 Improved Canny edge detection

Underwater imaging suffers from high noise, low contrast, and blurred details, but underwater terminal docking needs to capture image details accurately. Although the Canny algorithm is widely used in edge detection[15,16], the Gaussian filtering makes the edges smooth during denoising, and when the convolution kernel of the Sobel is small, the lower detection accuracy will result in false detection. To solve these problems, bilateral filtering instead of Gaussian filter denoising and the Scharr operator was used to extract the gradient.

Bilateral filtering[17] is an enhancement of Gaussian filtering that considers both the distance and the degree of similarity between pixels, preserving the main information characteristics of the image by avoiding blurring of the height difference part of each pixel, resulting in sharper edges. The formula for bilateral filtering is

$$\hat{f}(x,y)=\frac{\sum_{(i,j)\in S(x,y)} w(i,j)g(i,j)}{\sum_{(i,j)\in S(x,y)} w(i,j)}, \tag{1}$$

where $\hat{f}(x,y)$ is the pixel value after bilateral filtering; $g(i,j)$ is the pixel value; $S(x,y)$ is the value domain window of size $(2N+1)(2N+1)$; and $w(i,j)$ is the weighting factor. $w(i,j)$ can be expressed as

$$\begin{cases} w(i,j)=w_s(i,j)w_r(i,j), \\ w_s(i,j)=\exp\left(\dfrac{\left|g(i,j)-g(x,y)\right|^2}{2\delta_s^2}\right), \\ w_r(i,j)=\exp\left(\dfrac{\left|g(i,j)-g(x,y)\right|^2}{2\delta_r^2}\right), \end{cases} \tag{2}$$

where $w_s(i,j)$ is the spatial proximity factor, which decreases as the Euclidean distance between the target pixel and the center pixel increases; and $w_r(i,j)$ is the luminance similarity factor, which decreases as the

numerical difference between the target pixel and the center pixel increases.

The Scharr operator is an optimization of the Sobel operator for a kernel size of 3[18]. It assigns a higher weight to the central element, which can provide a stronger edge response and be able to accurately detect subtle changes in the image. In addition, it has the similar computational speed to Sobel but outperforms it in terms of accuracy and noise immunity. The Scharr operator formula is

$$\boldsymbol{G}_x=\begin{bmatrix}-3 & 0 & 3\\ -10 & 0 & 10\\ -3 & 0 & 3\end{bmatrix}\boldsymbol{I},\ \boldsymbol{G}_y=\begin{bmatrix}-3 & -10 & -3\\ 0 & 0 & 0\\ 3 & 10 & 3\end{bmatrix}\boldsymbol{I},$$
$$\boldsymbol{G}=\sqrt{\boldsymbol{G}_x^2+\boldsymbol{G}_y^2},\ \boldsymbol{\theta}=\arctan\left(\frac{\boldsymbol{G}_y}{\boldsymbol{G}_x}\right), \tag{3}$$

where $\boldsymbol{I}$ is the original image; $\boldsymbol{G}_x$ and $\boldsymbol{G}_y$ are the horizontal and vertical gradient directions, respectively; $\boldsymbol{G}$ is the gradient magnitude of the pixel; $\boldsymbol{\theta}$ is the gradient direction.

The original photo of the optical marker is shown in Fig. 3. The dispersion of the underwater light source is uneven, and there is a significant amount of background noise. The improved Canny algorithm performs better at preserving detail information while filtering and effectively reducing noise compared to the conventional Canny edge detection. The probability of missing genuine edges and misidentifying non-edges is reduced, leading in an overall improvement.

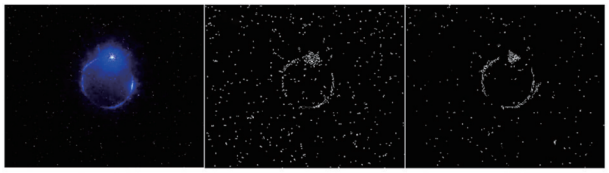

(a) Original image (b) Canny detection (c) Improved canny detection

Fig. 3 Comparison of edge detection

To further evaluate the proposed algorithm objectively, the peak signal-to-noise ratio (PSNR) and Platt's figure of merit (PFOM) are used for performance comparison. PSNR is a measure of the pixel difference between the signal and the noise by calculating the mean squared error (MSE), with larger values indicating better image quality. The formula for calculating PSNR is

$$\begin{cases} MSE=\dfrac{1}{mn}\displaystyle\sum_{i=0}^{m-1}\sum_{j=0}^{n-1}[\,I(i,j)-K(i,j)\,]^2,\\ PSNR=10\lg\left(\dfrac{\mathrm{MAX}_I{}^2}{MSE}\right),\end{cases} \tag{4}$$

where I and K are the original and processed images; m and n are the image size; MAX_I is the pixel maxima.

The PFOM is often used to evaluate the edge quality of a processed image, with larger values indicating that the ideal edge is closer to the actual edge. The formula for calculating PFOM is

$$PFOM=\frac{1}{\mathrm{MAX}(N_\mathrm{A},N_\mathrm{L})}\sum_{i=1}^{N_\mathrm{A}}\frac{1}{1+\alpha d_i^2}, \tag{5}$$

where N_A and N_L are the detected and ideal edges, respectively; d is the distance between them; and α is the compensation coefficient for misaligned edges.

The detected edges are compared with the edges in the original clean image, and the calculated results are shown in Table 1. Compared with the traditional Canny, the PSNR value of the improved Canny was increased by 2 dB, with better denoising ability; and the PFOM value was increased by 0.26, with higher accuracy of edge detection.

Table 1 Comparison of image metrics results

Method	PSNR	PFOM
Traditional canny	21.127	0.255
Improved canny	23.118	0.513

2.2 Adaptive threshold adjustment method

After acquiring the edge image, further threshold segmentation is needed to distinguish the light source marker from the background. As the AUV approaches the docking station, the light source marker is imaged in the camera from small to large gradually, and the brightness is from weak to strong. During dynamic detection, it is difficult to accurately distinguish between light sources and halos with a fixed threshold, and the selection of this threshold requires extensive experimentation. To solve this problem, an adaptive threshold method was proposed to optimize the detection of light source markers at different distances by dynamically adjusting the threshold in real-time. The flow of the adaptive threshold adjustment method is shown in Fig.4.

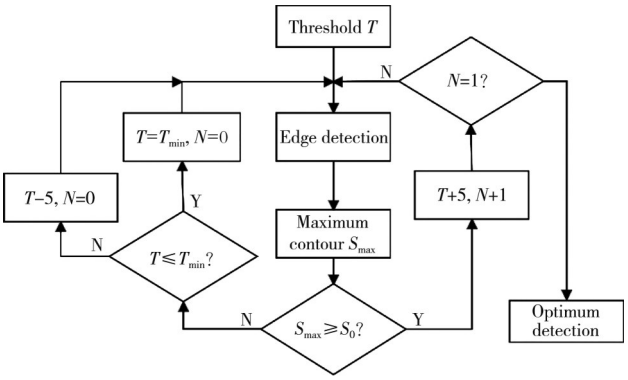

Fig. 4 Adaptive threshold adjustment process

The method designates the light source size at intermediate distance as a reference for estimating distance. When the target is far, the threshold gradually decreases to detect faint light sources. Conversely, when the distance gets closer, the threshold gradually increases to an optimal value for accurate detection of the light source region. Furthermore, this method incorporates a safety mechanism to prevent over-detection caused by a threshold that is set too low. The method gives priority to search when far away and priority to detect when near, thereby enhancing the detection and segmentation of underwater optical markers.

2.3 Light source interference elimination

Light source interference can appear in underwater images due to natural light, glowing objects, and environmental reflections. Especially in cases where the light source marker is bright or located in shallow water, reflections from the water surface can cause positioning interference and even cause docking failure. After image observation and analysis, reflections on water surfaces exhibit similar characteristics to the actual light source and always appear above the underwater light source.

To solve this problem, a method was proposed to eliminate the impact of interfering light sources based on the geometric positioning characteristics of the underwater light source marker. The largest closed contour was selected as the candidate light source area, and the lower-positioned one was selected as the target light source when contours of the same large area appeared. The underwater light source center selection process is shown in Fig.5.

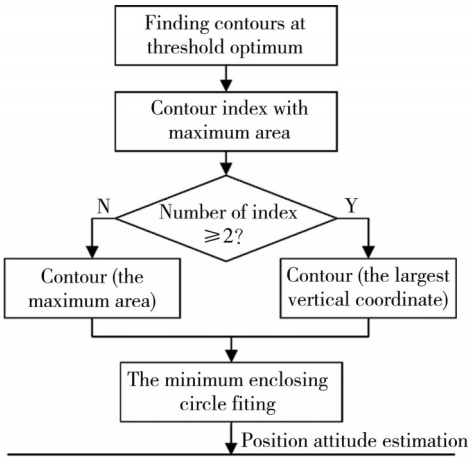

Fig. 5 Light source identification process

First, when the adaptive threshold was dynamically adjusted to the optimal threshold, the index and outermost point of each closed contour was captured one by one in the image, and its area and center coordinates are calculated sequentially. Then, a comparison was made and the contour index with the largest area among them was determined. If more than one maximal contour exists, the contour with the largest center longitudinal coordinate among them is selected as the target. Finally, the target contour was fitted with the minimum enclosing circle method to determine the underwater light source center point and radius for subsequent localization and attitude adjustment.

3 Position estimation and tracking

3.1 Camera calibration model

In the underwater optical mark detection and positioning by the AUV monocular visual guidance system, the reference coordinate system describes the relative position information[19]. This system consists of four coordinate systems: the world coordinate system, the camera coordinate system, the image pixel coordinate system, and the image physical coordinate system.

To convert feature points from the world coordinate system to the pixel coordinate system, conversion among four coordinate systems is required. The formula is

$$Z_c\begin{bmatrix}u\\v\\1\end{bmatrix}=\begin{bmatrix}1/\mathrm{d}x & 0 & u_0\\0 & 1/\mathrm{d}y & v_0\\0 & 0 & 1\end{bmatrix}\begin{bmatrix}f & 0 & 0 & 0\\0 & f & 0 & 0\\0 & 0 & 1 & 0\end{bmatrix}\begin{bmatrix}\boldsymbol{R} & \boldsymbol{t}\\\boldsymbol{0}^{\mathrm{T}} & 1\end{bmatrix}\cdot\begin{bmatrix}X_w\\Y_w\\Z_w\\1\end{bmatrix}=\begin{bmatrix}f_x & 0 & u_0 & 0\\0 & f_y & v_0 & 0\\0 & 0 & 1 & 0\end{bmatrix}\begin{bmatrix}\boldsymbol{R} & \boldsymbol{t}\\\boldsymbol{0}^{\mathrm{T}} & 1\end{bmatrix}\begin{bmatrix}X_w\\Y_w\\Z_w\\1\end{bmatrix}=\boldsymbol{M}_1\boldsymbol{M}_2\begin{bmatrix}X_w\\Y_w\\Z_w\\1\end{bmatrix}=\boldsymbol{M}\boldsymbol{X}, \tag{6}$$

where $\boldsymbol{M}$ is a 3×4 perspective projection matrix; and $\boldsymbol{X}$ is the coordinates of a point in space within the world coordinate system; $\boldsymbol{M}_1$ is determined only by the camera's internal parameters; while $\boldsymbol{M}_2$ is associated with the camera's position relative to the world coordinate system, and it is determined by the camera's external parameters.

In the process of converting the camera coordinate system to the image coordinate system, the image position is shifted due to camera distortion. According to the manufacturing accuracy and assembly process of the lens, the distortion is divided into radial distortion and tangential distortion. In this research, a professional underwater camera was used, the tangential aberration could be negligible, and the image correction was performed by de-distortion operation on the normalization plane. These camera parameters can be estimated by the camera

calibration, and the commonly used method is Zhang's plane calibration method[20]. Multiple calibration board images were taken with the camera from different angles, and then the parameters were calculated using the Matlab calibration toolbox. The camera calibration parameters are shown in Table 2.

Table 2 Camera calibration results

Parameters	Values
Internal parameter	$\begin{bmatrix} 1\,734.7 & 0 & 0 \\ 0 & 1\,735.1 & 0 \\ 997.836\,2 & 583.762\,1 & 1 \end{bmatrix}$
Radial distortion	(−0.271 8, −0.492 9, 0.127 8)

3.2 Monocular camera positioning

Euler angles can visually describe the attitude of the AUV, which are the roll, pitch and yaw rotating around its X, Y, and Z axes, respectively. The AUV can control the roll within less than 5°, resulting in the camera plane being approximately parallel to the docking plane. As shown in Fig. 6, when the AUV detects the light source marker and acquires its center coordinates, the orientation information of the AUV relative to the docking station can be calculated based on the deviation between the center of the image plane and the center of the light source marker.

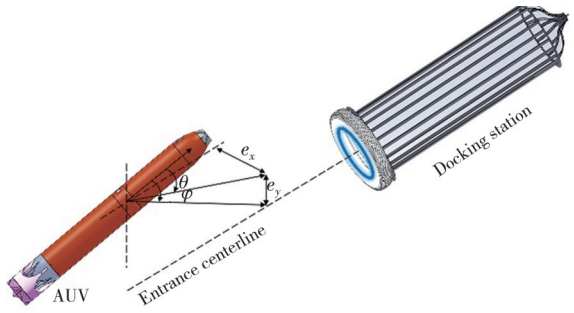

Fig. 6 Deviation adjustment of AUV docking attitude

The radius of the light source marker was R, the radius of the detection circle was r and the center was (u, v), and the camera's focal length f was 3.6 mm. Using the calibration model of the monocular camera and the geometric relation of perspective projection, the forward, horizontal, and vertical deviation distances (e_x, e_y, z) can be calculated by

$$\begin{cases} e_x = \dfrac{u - u_0}{f} z, \\ e_y = \dfrac{v - v_0}{f} z, \\ z = f \dfrac{R}{r}. \end{cases} \tag{7}$$

The horizontal and vertical adjustment angles (ψ, θ) of the AUV can be calculated by

$$\begin{cases} \psi = \arctan\left(\dfrac{e_x}{z}\right), \\ \theta = \arctan\left(\dfrac{e_y}{z}\right). \end{cases} \tag{8}$$

3.3 Position attitude controller

Due to the relatively short distance of the terminal docking, fast motion tracking processing based on the docking position is also required after visual inspection. Attitude regulation control of the AUV in the water is a complex and critical task. Compared with single-loop PID control, double-loop PID control has obvious advantages in dynamic response speed and overshoot reduction. Therefore, the outer loop was used to control the position of the AUV, while its attitude was controlled by the inner loop. The position attitude controller of the AUV is shown in Fig.7.

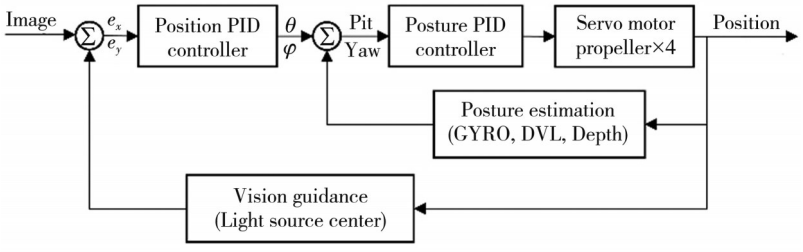

Fig. 7 AUV control block diagram

The horizontal and vertical offsets of the current AUV were used as inputs to the outer ring and were passed to the inner ring by the position PID controller to determine the current yaw angle and pitch angle. After processing the attitude estimation data of the integrated navigation system, the attitude PID controller output the speed and direction of the four motors. The integration of visual guidance and motion control allows the AUV to continuously adjust its horizontal yaw and vertical pitch direction while moving forward in the water, ensuring high controllability and efficiency.

As shown in Fig.8, the AUV set yaw angle is subjected

several large angular changes during the AUV docking process, and the tracking curve is able to be tracked quickly and continuously. As shown in Fig.9, the pit angle tracking curve quickly adapts to the complex changes in the preset heading curve with small estimation errors.

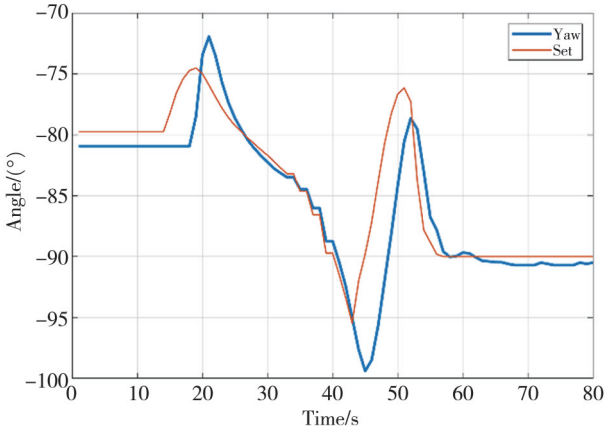

Fig. 8 AUV yaw tracking process

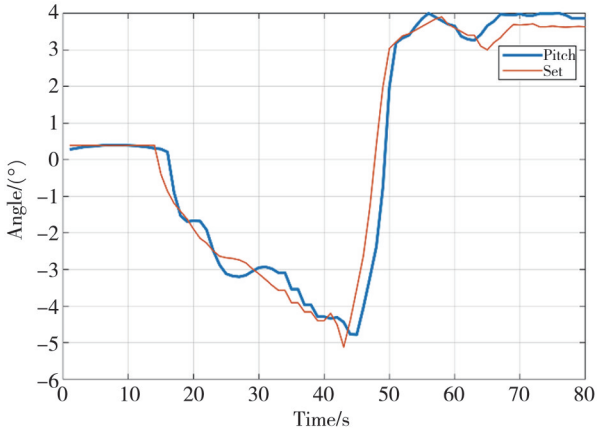

Fig. 9 AUV pit tracking process

The AUV is always stabilized at the correct direction and depth during yaw and pitch adjustments. This demonstrated that the position attitude control system could respond quickly and dynamically, track the target stably, and accurately realize the dual degree of freedom attitude adjustment of the AUV.

4 Pool experiment and analysis

To verify the effectiveness of the image processing and localization tracking methods, experimental validation in a pool is needed. The pool was 30 m long, 5 m wide, and 5 m deep. The docking station was smoothly placed in the center at the back of the pool, submerged at a depth of 2 m underwater, with the opening facing east at 90°. The AUV entered the underwater from the surface, dived to a certain depth, the AUV automatically leveled and stabilized its attitude and then completed the docking task independently using only monocular visual guidance.

In the pool docking experiment without light source interference, the process of AUV detection and tracking of light source markers is shown in Fig.10.

The red dot represents the center of the monocular camera image, while the green dot represents the center of the identified light source. The starting lateral position was about 1 m from the centerline of the docking station and the initial underwater depth was about 1.5 m, which resulted in the horizontal and vertical positions of the two dots not being aligned. However, the AUV continuously adjusted its attitude as it progressed, bringing the two center coordinate points closer together. Although the contour detected at a distance was larger than the actual light source area due to the lower threshold, the effect of the center deviation was small. The positioning accuracy in the middle and near distances played an important role in docking. As the AUV got closer, the detected contour got closer to the actual contour.

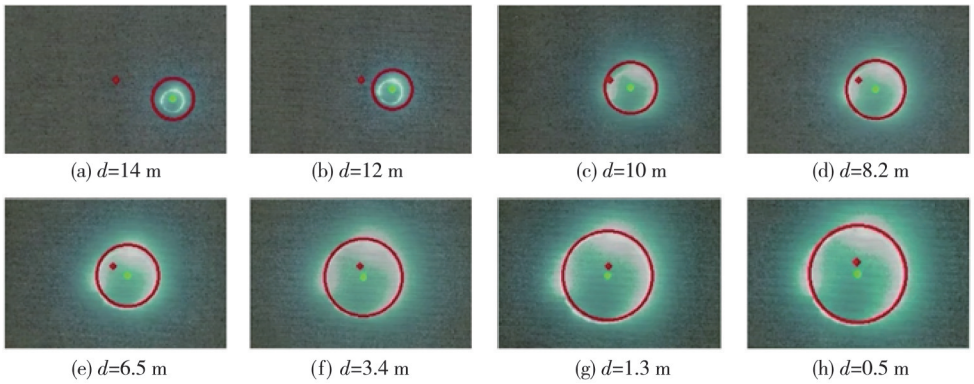

Fig. 10 AUV underwater docking process without light source interference

To evaluate the anti-interference ability of the visual guidance system, experiments were conducted where the brightness of the light source was increased. As shown in Fig.11, a bright region of the same brightness and size as the light source is formed on the water surface. It could be noticed that the visual detection range increased when the brightness of the light source was enhanced.

In the docking process, the AUV successfully identified and tracked the correct underwater light source marker from a distance. At close range, the AUV accurately segmented the actual light source from the highlighted area with high localization accuracy. The AUV was not misguided in a disturbed environment and entered the docking station, which proved that the monocular visual guidance was robust.

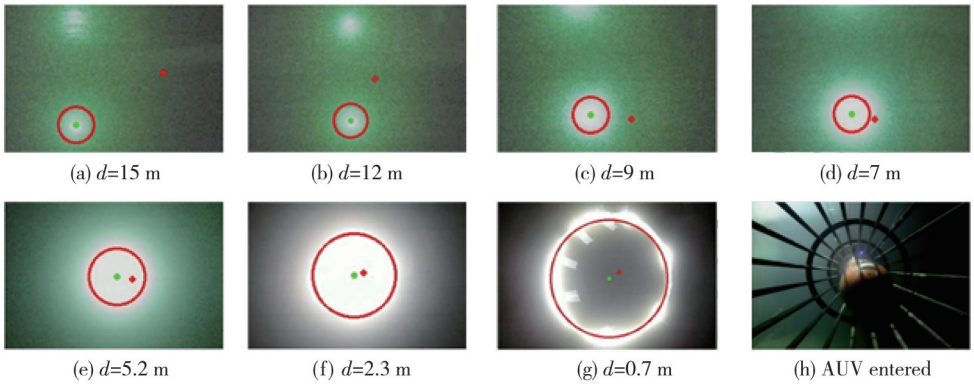

Fig. 11 AUV underwater docking process with light source interference

During the underwater monocular guided docking, the AUV was able to detect up to 15 m, the heading angle adjustment deviation of 10°, and a depth adjustment deviation of 0.5 m. The AUV navigated at a speed of 0.41 m/s, and the docking took about 40 s. The center of the image light source was precisely positioned and processed at a rate of more than 25 frames per second. The AUV carried out 15 experiments in each of the two docking scenarios, and successfully docked 14 times and 13 times, respectively, with an overall docking success rate of 90%. It showed that in a complex underwater environment full of noise and interference, the visual guidance method had an efficient and accurate docking recovery capability.

5 Conclusions

A simple and reliable solution was presented for AUV terminal docking. For the individual light source marker, the enhanced Canny algorithm was used to improve the edge detection accuracy, the adaptive threshold was used to improve the applicability, and the light source interference cancellation was used to improve the anti-interference capability. The AUV used heading and pitch deviation for position-attitude estimation, which did not require complex source identification and localization algorithms. The position-attitude PID controller could realize stable and continuous attitude tracking. The pool experiment verified the effectiveness of this monocular visual guidance, which provided technical support for the AUV deployment and recoveried in the marine environment.

Acknowledgement

This research was supported by Special Fund for Science and Technology Innovation Teams of Shanxi Province (No. 202304051001030).

Declaration of conflicting interests

The authors have no conflict of interests related to this publication.

References

[1] BOGUE R. Underwater robots: a review of technologies and applications. Industrial Robot, 2015, 42(3): 186-191.
[2] BOROVIK A I, RYBAKOVA E I, GALKIN S V, et al. Experience of using the autonomous underwater vehicle MMT-3000 for research on benthic communities in antartica. Oceanology, 2022, 62(5): 709-720.
[3] RUMSON A G. The application of fully unmanned robotic systems for inspection of subsea pipelines. Ocean Engineering, 2021, 235: 109214.
[4] WIBISONO A, PIRAN M J, SONG H K, et al. A survey on unmanned underwater vehicles: challenges, enabling technologies, and future research directions. Sensors, 2023, 23(17): 7321.
[5] LIN M W, LIN R, YANG C J, et al. Docking to an underwater suspended charging station: systematic design and experimental tests. Ocean Engineering, 2022, 249: 110766.
[6] VANDAVASI B N J, VENKATARAMAN H, GIDUGU A R. Machine learning-based electro-magnetic field guided localization technique for autonomous underwater vehicle homing. Ocean Engineering, 2023, 280: 114692.
[7] CONG Y, GU C, ZHANG T, et al. Underwater robot sensing technology: a survey. Fundamental Research, 2021, 1(3): 337-345.
[8] YAZDANI A M, SAMMUT K, YAKIMENKO O, et al. A survey of underwater docking guidance systems. Robotics and Autonomous Systems, 2020, 124: 103382.
[9] SONG L, HOU Y P, ZHANG J P, et al. Monocular

visual 3D cuboid measurement method based on Mask-RCNN and SFM. Journal of Measurement Science and Instrumentation, 2023, 14(2): 127-136.
[10] PARK J Y, JUN B H, LEE P M, et al. Experiments on vision guided docking of an autonomous underwater vehicle using one camera. Ocean Engineering, 2009, 36(1): 48-61.
[11] BIANCHI FIGUEIREDO A, COIMBRA MATOS A. MViDO: A high performance monocular vision-based system for docking a hovering AUV. Applied Sciences, 2020, 10(9): 2991.
[12] PALOMERAS N, VALLICROSA G, MALLIOS A, et al. AUV homing and docking for remote operations. Ocean Engineering, 2018, 154: 106-120.
[13] LI D J, ZHANG T, YANG C. Terminal underwater docking of an autonomous underwater vehicle using one camera and one light. Marine Technology Society Journal, 2016, 50(6): 58-68.
[14] LIU S, OZAY M, OKATANI T, et al. Detection and pose estimation for short-range vision-based underwater docking. IEEE Access, 2019, 7: 2720-2749.
[15] ZHAO L J, ZHU R S. Research on image contour edge analysis based on canny edge detector. Academic Journal of Computing & Information Science, 2022, 5(1): 70-75.
[16] FENG Y, HAN B, WANG X, et al. Self-supervised transformers for unsupervised sar complex interference detection using canny edge detector. Remote Sensing, 2024, 16(2): 306.
[17] RUHELA R, GUPTA B, LAMBA S S. An efficient approach for texture smoothing by adaptive joint bilateral filtering. The Visual Computer: International Journal of Computer Graphics, 2023, 39(5): 2035-2049.
[18] LI Q, MENG H, LI Y. Texture-based fast QTMT partition algorithm in VVC intra coding. Signal, Image and Video Processing, 2023, 17(4): 1581-1589.
[19] FU L H, WANG C Y, HE J J, et al. Camera pose measurement method based on feature matching. Journal of Measurement Science and Instrumentation, 2023, 14(1): 1-8.
[20] ZHANG Z Y. A flexible new technique for camera calibration. IEEE Transactions on Pattern Analysis and Machine Intelligence, 2000, 22(11): 1330-1334.

AUV终端对接的单目视觉导引方法研究

王秋生, 齐向东*, 薛晨阳, 刘　丹, 王永华, 王景楠

中北大学 仪器科学与动态测试教育部重点实验室, 山西 太原 030051

摘　要: 在水下复杂环境中高效回收自主潜水器(AUV)是一项重大的技术挑战。本文提出了一种利用单目视觉检测和跟踪对接站上光环标识进行终端对接的方法。为了提高光源特征识别, 本文改进了Canny边缘检测算法, 采用自适应阈值方法动态调整光源轮廓, 并在阈值最优时采用最小外接圆方法确定光源中心。此外, 利用几何位置和面积约束消除水面反射的干扰。在视觉定位和跟踪方面, 采用张氏标定法获取相机的内部参数和畸变参数, 通过比较光环中心和图像中心来估计AUV的航向和俯仰偏差, 然后利用位置-姿态PID控制器进行快速跟踪。水池实验结果表明, 该方法简单实用, 鲁棒性强, 能够为未来水下机器人的可靠回收提供一定技术参考。

关键词: 自主潜水器(AUV); 终端对接; 单目视觉; 位姿估计; 图像处理

引用格式: WANG Qiusheng, QI Xiangdong, XUE Chenyang, et al. Monocular visual guidance method for terminal docking of an autonomous underwater vehicle. Journal of Measurement Science and Instrumentation, 2024, 15(2): 216-223.